JMEPEG (2004) 13:600-606
DOI: 10.1361/10599490420610

1059-9495/$19.00

Critical Level of Intergranular Fracture to Affect the Toughness of Embrittled 2.25Cr-1Mo Steels

M.A. Islam, J.F. Knott, and P. Bowen

(Submitted October 28, 2003)

In general, the low-temperature brittle fracture mode of unembrittled ferritic steel is transgranular cleavage. During temper embrittlement, impurity elements, such as sulfur (S), phosphorus (P), antimony (Sb), arsenic (As), and tin (Sn), segregate to prior austenite grain boundaries, which results in a decrease in the grain boundary cohesive strength. As a result, the brittle transgranular cleavage fracture mode changes to intergranular decohesion in association with the decrease in the critical fracture stress (σ_F) as well as the fracture toughness (K). However, the appearance of intergranular facets on the fracture surface does not cause a decrease in the K and σ_F values. In this work, quenched and fully tempered 2.25Cr-1Mo steel (in an unembrittled condition that exhibits almost 100% brittle transgranular cleavage fracture) has been embrittled for 24, 96, and 210 h at 520 °C to produce different proportions of intergranular fracture. These unembrittled and embrittled steel specimens were tested to measure K (at −120 and −196 °C) and σ_F (at −196 °C). The experimental results and detailed fractographic observations show that the K and σ_F values decrease with an increase in the area fraction of intergranular fracture, provided that the area fraction of the intergranular facet on the brittle fracture surface exceeded a certain critical level, approximately 20-22%.

Keywords brittle fracture, embrittlement, fracture stress, fracture toughness, segregation

1. Introduction

Chromium-molybdenum (Cr-Mo) low alloy steels are widely used for the electric-power-generating and petrochemical industries because they possess excellent mechanical properties, especially fracture toughness (K), over a wide range of temperatures.[1,2] Due to their cost-effectiveness and good combination of strength and toughness in the quenched and tempered (QT) condition, 2.25Cr-1Mo steel is a popular candidate for these applications in the family of Cr-Mo low alloy steels. However, the susceptibility of the alloy to temper embrittlement due to the segregation of trace elements is high and is of great concern when designing critical parts.

The brittle fracture mode of unembrittled (i.e., QT condition) ferritic low alloy steel is transgranular cleavage, but this fracture mode can be changed if the grain boundary impurity element segregation exceeds a certain level. So, after embrittlement, the brittle fracture mode may be either mixed (transgranular cleavage and intergranular decohesion) or fully intergranular, depending on the degree of grain boundary segregation. Segregation not only changes the fracture mode but can also adversely affect the fracture resistance of the steel, provided that the proportion of intergranular facets exceeds a certain critical value. However, it should be noted that limited work has been done so far on this subject. The aim of this work was to produce different proportions of intergranular fracture by employing suitable heat treatment cycles and then to determine the minimum level of intergranular fracture that can cause a significant change in the toughness of the steel.

M.A. Islam, Materials and Metallurgical Engineering Department, Bangladesh University of Engineering and Technology (BUET), Dhaka-1000, Bangladesh; and **J.F. Knott** and **P. Bowen,** School of Metallurgy and Materials, The University of Birmingham, B15 2TT, Edgbaston Birmingham, UK. Contact e-mail: aminulislam@mme.buet.ac.bd.

2. Experimental

2.1 Materials and Heat Treatment

All tests were performed on a commercial grade of 2.25Cr-1Mo steel plate of the composition given in Table 1. Single edge notch bend (SENB) testpieces of dimensions 10 × 15 × 70 mm^3 (for K measurements) and specimens of geometry shown in Fig. 1 (for σ_F measurements) were machined and encapsulated in silica glass tubes under an inert atmosphere. All testpieces were austenitized for 2 h at a temperature of 1100 °C in a furnace with a temperature control of ±4 °C. The samples then were quenched in oil. These quenched specimens were tempered for 2 h at 650 °C and then again were quenched in oil. Some of these QT specimens were aged at 520 °C for 24, 96, and 210 h. The details of the heat treatment conditions are given in Table 2.

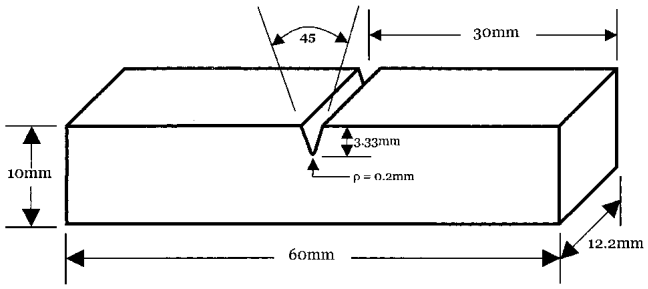

Fig. 1 Blunt notch specimen geometry

Table 1 Chemical composition of the steel

Composition, wt.%													
C	Si	S	P	Mn	Ni	Cr	Mo	V	Cu	Al	Co	Nb	Ti
0.15	0.22	0.023	0.013	0.51	0.11	2.27	0.91	0.01	0.16	0.03	0.01	0.003	0.004

Table 2 Heat treatment conditions

Serial number	HT conditions	HT codes
1	1100 °C/2 h/OQ + 650 °C/2 h/OQ	QT
2	1100 °C/2 h/OQ + 650 °C/2 h/OQ + 520 °C/24 h/OQ	QTLE
3	1100 °C/2 h/OQ + 650 °C/2 h/OQ + 520 °C/96 h/OQ	QTME
4	1100 °C/2 h/OQ + 650 °C/2 h/OQ + 520 °C/210 h/OQ	QTHE

Note: HT, heat treatment; OQ, oil quenched

Table 3 Resulted mean carbide sizes of the steel under different heat treatment conditions

Heat treatment code	Size of carbide particles, μm	
	Length	Width
QT	0.60 ± 0.42	0.30 ± 0.25
QTLE	0.63 ± 0.45	0.36 ± 0.32
QTME	0.67 ± 0.50	0.38 ± 0.30
QTHE	0.70 ± 0.46	0.40 ± 0.22

2.2 Metallography

Polished metallographic samples of all heat treatment conditions were etched in 2% nital and were observed using optical microscopy. For carbide size distributions, scanning electron microscope (SEM) observations were made on all specimens at a 0° tilt and were photographed at 2000×. Using these SEM micrographs, quantitative measurements of carbide sizes were made using an image analyzer.

2.3 Tensile Testing

Tensile testing was carried out on a computer-controlled universal testing machine at −196 °C in air. All tensile tests were performed using a crosshead displacement of 1mm/min with load-elongation diagrams obtained automatically from the computer.

2.4 Fracture Toughness and Fracture Stress Measurement

K specimens were prepared and tested using a three-point bend configuration at −120 and −196 °C according to BS7448.[3] For all heat treatment conditions, *K* tests were repeated on sets of 10 specimens. The values of *K* then were calculated using:

$$K = \frac{F\,S}{BW^{1.5}} f(a_o/W)$$

where F, B, W, S, a_o, and f (a_o/W) are, respectively, relevant load at brittle fracture, specimen thickness, specimen width, span, effective crack length, and the compliance function of the specimen.

Using the same machine, sets of five specimens of the geometry shown in Fig. 1 were tested at −196 °C following the analysis of Griffiths and Owen[4] for fracture stress (σ_F) measurement.

2.5 Fractography

After the mechanical tests for *K* and σ_F measurements, fracture surfaces were extracted and cleaned. Fractographic observations were carried out in the SEM operating at 20 kV and a 0° tilt. Using these SEM micrographs, the area fraction of intergranular fracture was measured either manually or automatically using an image analyzer.

3. Results and Discussion

3.1 General Observation

The micrographs on the polished and nital-etched specimens under all heat treatment conditions were produced using optical microscopes and SEMs. QT specimens showed a tempered martensitic structure with distributed carbide particles. The aging of the QT specimens at 520 °C caused no significant change in the microstructure; however, a gradual increase (very slight) in carbide sizes was observed (Table 3). A typical tempered martensitic structure and the distribution of carbide particles in the microstructure are shown in Fig. 2. It is to be noted that there are many more carbide particles of submicron size that were not resolved at this magnification. So, the sizing of carbides by SEM is only for a comparative study among the different heat treatment conditions.

The 0.2% proof stress at −120 °C and −196 °C for the specimens for all heat treatment conditions are presented in Table 4. From this table, it is clear that embrittlement has no marked effect on the tensile behavior of QT specimens.

The average *K* values of sets of 10 specimens at subambient temperatures for the different heat treatment conditions are presented in Table 5. After full tempering (i.e., 2 h at 650 °C), QT specimens were embrittled isothermally at 520 °C for different time periods. Isothermal embrittlement at 520 °C for 24 h (i.e., the QTLE condition) reduced the average *K* value of the QT condition, and also the *K* values were found to be a function of embrittlement time (QTME condition, 96 h; QTHE condition, 210 h).

σ_F measurements were carried out only at −196 °C on sets of five specimens in each heat treatment condition. The average σ_F values of QT, QTLE, QTME, and QTHE conditions are presented in Table 6. From this table, it is clear that σ_F values follow a very similar trend to that of *K* values.

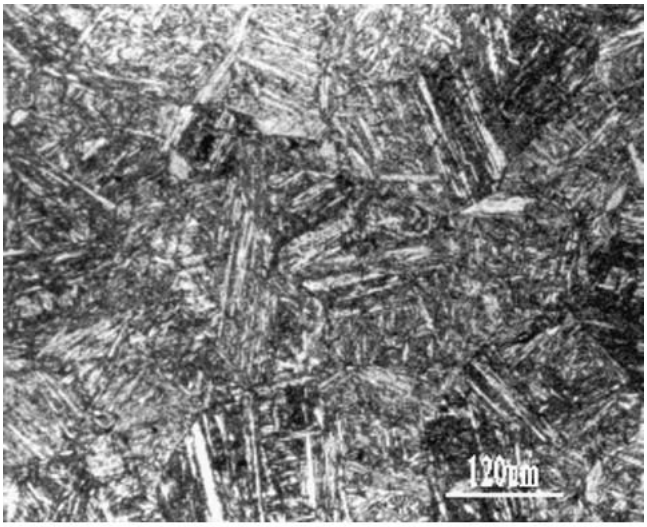

(a)

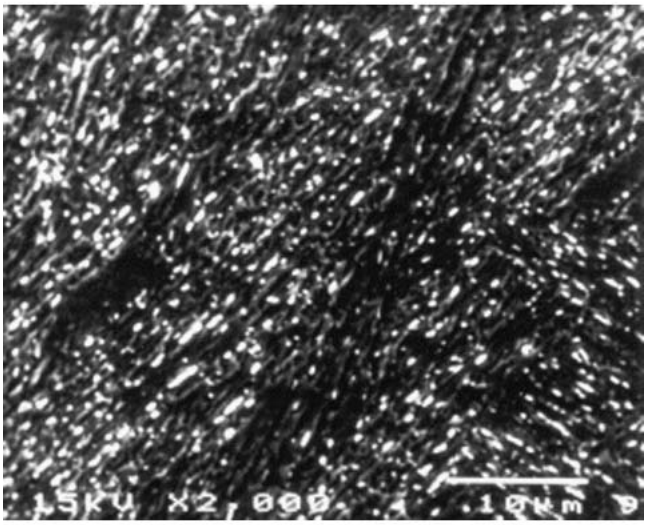

(b)

Fig. 2 Microstructure of the QTLE specimen: (**a**) an optical micrograph showing the QT martensitic structure; (**b**) SEM micrograph showing the distribution of carbide particles

Table 4 Resulted 0.2% proof stresses at −196 °C

Heat treatment code	0.2% proof stress, MPa
QT	1180
QTLE	1180
QTME	1170
QTHE	1140

Both the QT and QTLE conditions possessed similar yield stresses. Compared with those for the QT specimens, the carbide particles in the QTLE specimens were slightly coarser and the impurity segregation level was significantly higher (Table 7). It also should be noted that the segregated element for this heat treatment condition is mainly P, and the P segregation is measured in terms of the percentage of peak height ratio (%PHR) of P (P_{120}/Fe_{703}).[5-8]

Table 5 Average *K* values and percentage intergranular fracture at −120 °C and −196 °C

	At −120 °C		At −196 °C	
HT code	*K*	%IGF	*K*	%IGF
QT	71.3	Nil	45.5	Nil
QTLE	66.4	26.0	42.1	19.0
QTME	60.3	44.0	36.1	39.0
QTHE	53.0	71.0	32.1	65.0

Note: HT, heat treatment; %IGF, percentage intergranular fracture

The QT specimen exhibited brittle transgranular cleavage fracture (Fig. 3). The higher segregation level in the QTLE condition changed the fracture mode of the QT condition to a mixed fracture mode that was characterized by transgranular cleavage and intergranular decohesion (Fig. 4). When the impurity element segregation level at the grain boundaries exceeds a critical threshold value, the fracture mode changed from transgranular cleavage to intergranular decohesion. The decrease in the value of *K* is arguably due to the higher level of impurity segregation, which changes the fracture mode. The average *K* value for the QTME condition is lower than that for the QTLE condition (Table 5). The specimens for the QTLE and QTME conditions have the same level of yield stress, but the segregation level for the QTME condition is much higher (Table 7). The average proportion of intergranular fracture has now increased from 20-25% to 40-45%. From Table 5, it is clear that the QTHE condition resulted in a further decrease in the average value of *K*. The reason for this is the much higher exposure time during embrittlement, which caused additional impurity segregation. The presence of secondary intergranular cracking on the fracture surface of QTHE specimen is also an indication of the higher level of P segregation at grain boundaries (Fig. 5). The higher segregation level also resulted in a higher proportion of intergranular fracture and in lower *K* values. The general observations of toughness deterioration in terms of σ_F for different heat treatment conditions explored the same trend as that of toughness values (Tables 5, 6).

3.2 Critical Level of Intergranular Fracture

In Fig. 6, all *K* values (10 values for each condition) for the QT, QTLE, QTME, and QTHE conditions, at both −120 and −196 °C, are plotted versus the corresponding area fractions of intergranular facet (i.e., at a distance >7 mm from the fatigue crack tip). This figure shows that the *K* value decreases with an increase in the area fraction of intergranular fracture, as discussed earlier. From Fig. 6, an important observation is that the *K* values start to decrease significantly (beyond the scatter band for QT specimens, which exhibited 100% transgranular cleavage fracture) when the area fraction of intergranular facets on the fracture surface exceeds a critical level. The horizontal lines corresponding to the highest and the lowest *K* values, as determined by the bounds of toughness at the 0% intergranular facet, intersects the *K* value versus the percentage of intergranular fracture curve at approximately 20-22% for both low

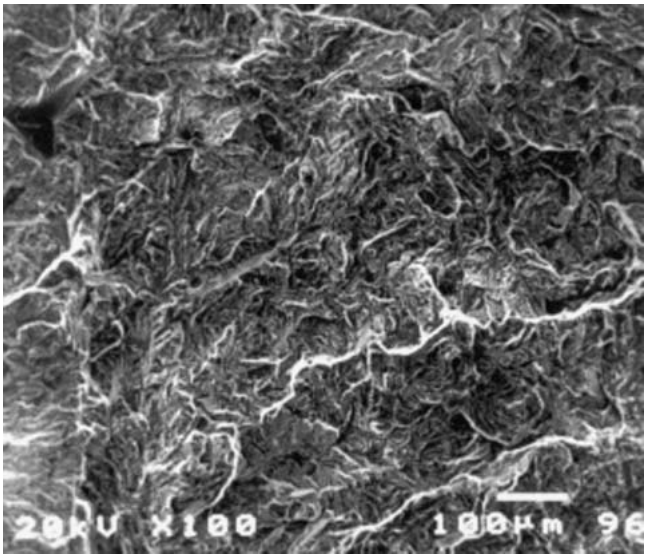

Fig. 3 Almost completely transgranular cleavage fracture on the QT specimen

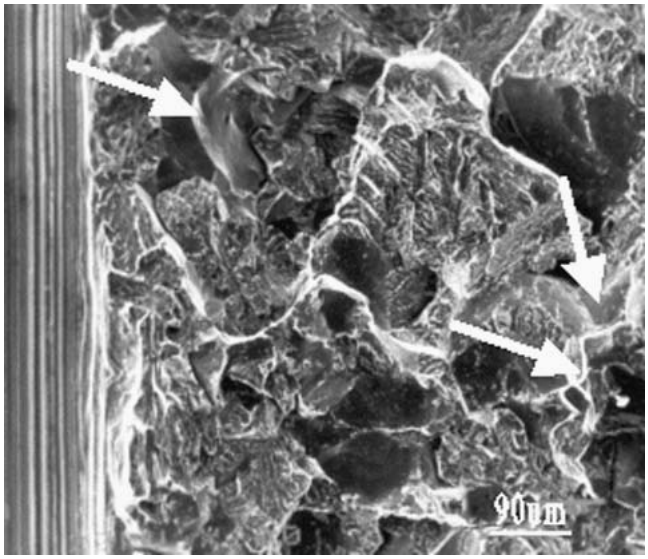

Fig. 4 SEM micrograph of the QTLE specimen showing a mixed-mode (i.e., transgranular cleavage and intergranular decohesion type fracture) of fracture. Intergranular facets are marked by arrows.

Table 6 Average σ_F values and percentage intergranular fractures at −196 °C

HT code	σ_F, MPa	%IGF
QT	2941	~0
QTLE	2874	21
QTME	2642	47
QTHE	2499	68

Note: HT, heat treatment; %IGF, percentage intergranular fracture.

Table 7 The AES %PHR (average) of P (P_{120}/Fe_{703})

HT code	P
QT	(a)
QTLE	11.4 ± 1.5
QTME	15.6 ± 1.7
QTHE	18.8 ± 1.8

(a) No intergranular fracture was found to analyze in AES.

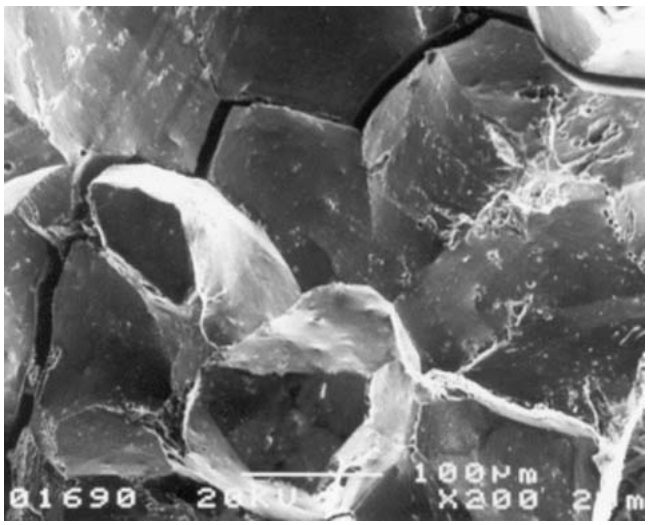

Fig. 5 Very clean-cut secondary intergranular cracking observed on QTHE specimen. Note: the brittle fracture mode is almost entirely of the intergranular decohesion type.

temperatures. Figure 7 shows the relationship between the proportion of intergranular facets observed on different specimens and σ_F values of QT, QTLE, QTME, and QTHE conditions tested at −196 °C. From this figure, a similar observation to the one observed for K (Fig. 6) is evident.

It is now well documented that impurity element segregation lowers the local intergranular cohesive strength, and, as a result, the microscopic σ_F decreases. On the other hand, K is dependent on the local σ_F of the material. In the present investigation, a direct relationship between microscopic σ_F and K values has been observed (Tables 5, 6), and, thus, knowing the relationship of the percentage of intergranular facets with K and σ_F will be helpful in understanding this behavior.

Consider the experimental results for K and microscopic σ_F values. For the measurement of K, 10 specimens in each condition were tested at both −120 and −196 °C. These results give more information than the σ_F results, for which only five specimens in each condition were tested. However, it is to be noted that the observed trends are similar for both K and σ_F, even though a limited number of specimens have been tested for σ_F measurement (Fig. 6 and 7). According to the experimental K values and the corresponding proportions of intergranular facets observed on the fracture surfaces, it is clear that the K and/or σ_F are not influenced up to a certain level of intergranular fracture. Consequently, the following observations were made:

- The grain boundaries are stronger than the cleavage planes in the unembrittled steel.[9,10]

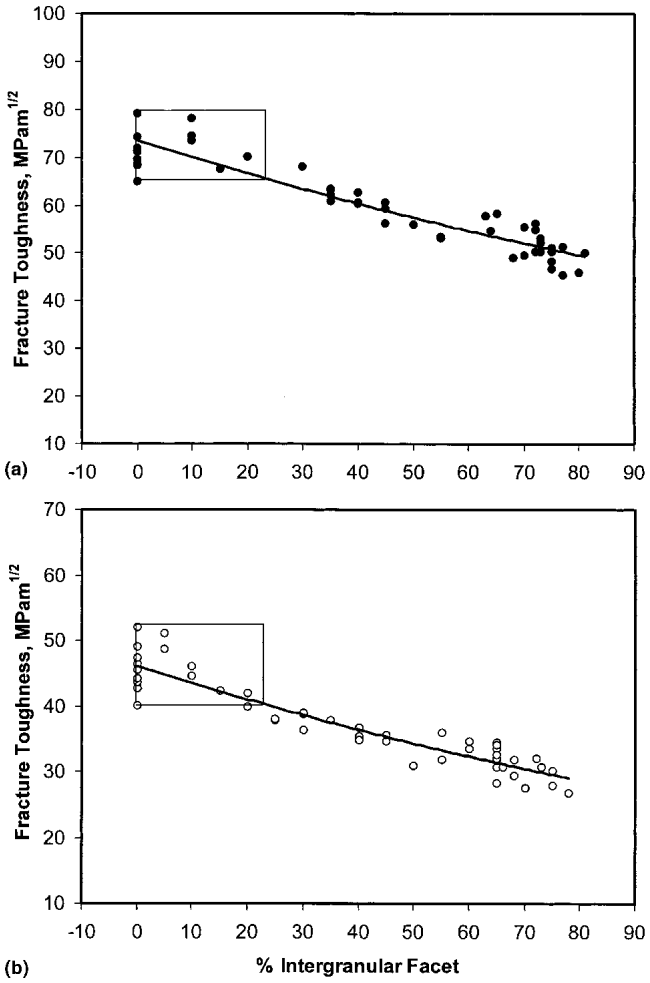

Fig. 6 K versus the percentage of intergranular fracture (**a**) at −120 °C and (**b**) at −196 °C

- With an increase in the grain boundary impurity coverage, the percentage of intergranular fracture increases and the local σ_F decreases.[5,7,11] (Here it is to be noted that the intergranular facets observed are mainly due to P segregation.[5-8])

Consider first the features of cleavage fracture. Cleavage fracture is a rapid propagation of a crack along a particular crystallographic plane. In the case of body-centered cubic (bcc) materials, cleavage occurs on {100} planes.[10] The cleavage planes in the unembrittled condition are weaker than the grain boundary cohesive strength of the steel.[9,10] This situation is shown in the schematic diagram in Fig. 8(a). As a result, transgranular cleavage is the typical brittle mode of fracture in ferritic low alloy steels. Temper embrittlement causes impurity segregation to prior austenite grain boundaries and reduces the intergranular cohesive strength, as shown in Fig. 8(b). However, this level of grain boundary segregation is insufficient to change the fracture mode from transgranular cleavage to intergranular decohesion, because the intergranular cohesive strength is still well above the cleavage strength. The change in the fracture mode becomes apparent when the segregation reduces the intergranular cohesive strength level to values equal to or lower than the cleavage strength for the unembrittled material. This phenomenon is shown in Fig. 8(c). It has been explained that the segregation is a complex phenomenon, and, in general, impurity elements segregate to the most favored sites.[12] When the segregation level of a certain set (i.e., "the most disordered") of grain boundaries exceeds the threshold value, they start to fail by intergranular decohesion. With exposure time, if the segregation levels of the other boundaries exceed this threshold value, then they too will fail by intergranular decohesion, and gradually the proportion of intergranular fracture will increase.

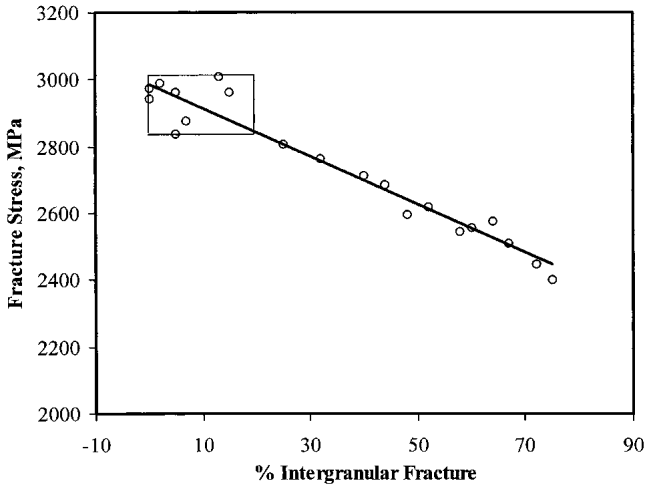

Fig. 7 Fracture stress versus the percentage of intergranular fracture at −196 °C

Now consider the segregation-induced σ_F reduction. From the above discussion, it is clear that the brittle transgranular cleavage fracture mode can be changed to intergranular decohesion, if the grain boundary segregation reduces the grain boundary strength level to values equal to or below the strength of the cleavage plane. It is, therefore, concluded that the occurrence of some proportion of intergranular fracture does not necessarily imply a reduction of σ_F and K values, because only at a critical level of impurity segregation does the grain boundary strength approach that of the cleavage plane (Fig. 8c). The reduction in intergranular fracture strength below the transgranular cleavage fracture strength becomes apparent only when segregation reduces the grain boundary strength significantly compared with the strength of the cleavage plane. This implies that the required level of impurity segregation for the occurrence of intergranular fracture and the reduction in the intergranular σ_F are not the same, and, arguably, the latter needs a higher level of segregation. The presence of a certain level of impurity element (such as P) coverage at prior austenite grain boundaries and its ability to affect the σ_F value has been noted.[5,11] Briant and Banerji[13] studied the embrittling effect on the cleavage the σ_F of Ni-Cr steel. For this steel, they found the threshold level to be a 20% P monolayer coverage. Below this value, the σ_F was independent of the level of segregated impurities. Naudin et al.[11] found the threshold level to be ~10% P monolayer coverage (equivalent to ~20% intergranular fracture) for Mn-Ni-Mo-Cr steel (A508, Class 3). A

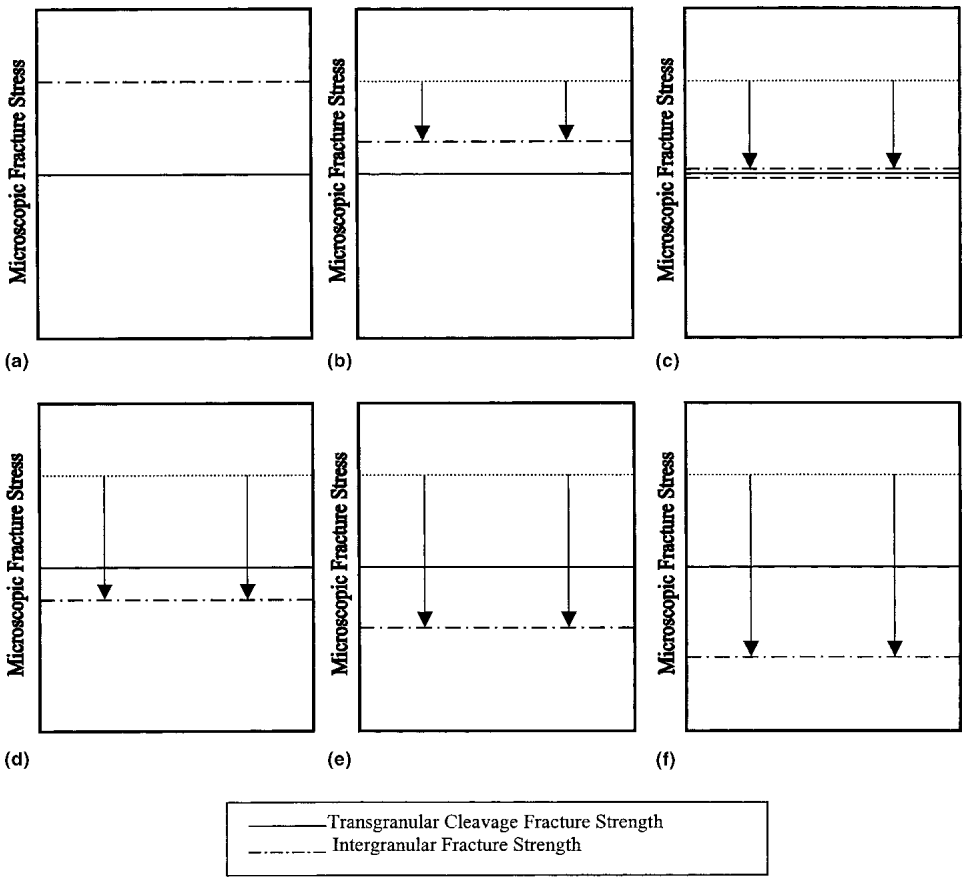

Fig. 8 Schematic representations showing the variation of intergranular cohesive strength with impurity element coverage

theoretical analysis by Smith et al.[14] predicted that with intergranular strength equal to transgranular cleavage strength, about 20% intergranular fracture would be expected. However, the value of the threshold level of impurity element segregation and/or the proportion of intergranular fracture may vary, and this difference is related to the variation in the alloying elements.[11]

It has been suggested that impurity elements first start to segregate to the most favorable sites,[12] and, with time, the segregation level at these sites plausibly exceeds the minimum level to cause intergranular fracture. If the impurity elements are further allowed to segregate, the work-of-fracture of these boundaries will be significantly lower than the transgranular cleavage work-of-fracture. In the meantime, the segregation level of some comparatively less favorable sites (grain boundaries) also will exceed the threshold level for intergranular fracture. The first effect causes the σ_F to decrease, while the second effect gives rise to an increased proportion of intergranular fracture. Both effects are linked, so σ_F decreases as the proportion of intergranular fracture increases.

Now consider the individual heat treatment conditions that were used for the present investigation. QT specimens exhibited almost 100% transgranular brittle fracture. This suggests that the grain boundary segregation level of QT specimens (if there is any segregation) is below the threshold level to cause intergranular brittle fracture. This behavior is analogous to the situation in Fig. 8(b). For QTLE specimens, QT specimens were isothermally embrittled for 24 h at 520 °C. During the 24 h of exposure, more impurity elements could segregate to prior austenite grain boundaries. This is supported by Auger electron spectroscopy (AES) results (Table 7). For these conditions, the grain boundary segregation level not only exceeded the level needed to give intergranular decohesion, but for some specimens grain boundaries in the high-stress area ahead of the notch experienced a segregation level sufficient to cause a noticeable decrease in the grain boundary strength. As a result, the σ_F starts to decrease, as pictured in Fig. 8(d). Due to the complex nature of segregation and to the local variations in composition and microstructures, grain boundaries in some QTLE specimens also may have a segregation level that is very close to the threshold level needed to cause intergranular decohesion (Fig. 8c). As a result, no significant reduction either in σ_F or K values was observed, even though the specimens exhibited a marked proportion of intergranular fracture.

With further aging (i.e., 96 h, the QTME condition, and 210 h, QTHE condition), the segregation level of all grain boundaries increased. Coupled with this was a subsequent decrease in the intergranular cohesive strength. These situations are shown in Fig. 8(e) and (f). More boundaries, thus, reach the threshold value for the occurrence of intergranular decohesion. As a result, the percentage of intergranular fracture increases with a subsequent decrease in microscopic σ_F and K values.

4. Conclusions

As evidenced by the fractographic observation of embrittled specimens, in which the fracture mode is mixed (i.e., transgranular cleavage and intergranular decohesion), a correlation was found between the proportion of intergranular facets and the corresponding K or σ_F values.

The comparison of experimentally observed K values and fractographic observations showed that a proportion of intergranular facets of less than 20-22% does not decrease the K value. This experimental observation suggests that for mixed-mode fracture, with less than 20-22% intergranular facets, the intergranular work-of-fracture resulting from the corresponding level of segregation is possibly greater than or equal to that for transgranular cleavage work-of-fracture.

References

1. R.C. Thomson and M.K. Miller, Carbide Precipitation in Martensite During the Early Stages of Tempering in Cr and Mo-Containing Low Alloy Steels, *Acta Mater.,* Vol 46 (No. 6), 1998, p 2203-2213
2. R. Pilkington, R. Dicken, P. Peura, G.M. Lorimer, G.C. Allen, M. Holt, and C.M. Younes, Trace Element Embrittlement in 2.25%Cr-1%Mo Steel, *Mater. Sci. Eng.,* Vol A212, 1996, p 191-205
3. "Fracture Mechanics Toughness Tests, Part 1, Method for Determination of K_{IC}, Critical CTOD and Critical J Values of Metallic Materials," BS 7448, 1991, p 2677-2710
4. J.R. Griffiths and D.R.J. Owen, An Elastic-Plastic Stress Analysis for a Notched Bar in Plane Strain Bending, *J. Mech. Phys. Soc.,* Vol 19, 1971, p 419-431
5. M.A. Islam, "Intergranular Fracture in 2.25Cr-1Mo Pressure Vessel Steel," Ph.D. Thesis, The University of Birmingham, UK, 2001
6. M.A. Islam, P. Bowen, and J.F. Knott, Grain Boundary Fracture Processes in Quenched and Tempered Structural Steels, Proceedings of a Workshop (Birmingham University, UK), 16-17 Sept 1999, p 55-72
7. M.A. Islam, J.F. Knott, and P. Bowen, Low Temperature Fracture Toughness of Embrittled 2.25Cr-1Mo Pressure Vessel Steel, *Advances in Mechanical Behaviour, Plasticity and Damage,* 7-9 Nov 2000 (Tours, France), Elsevier Science Ltd., Vol 2, p 1415-1420
8. M.A. Islam, M. Novovic, P. Bowen, and J.F. Knott, Effect of Phosphorus Segregation on Fracture Properties of 2.25Cr-1Mo Pressure Vessel Steel, *J. Mater. Eng. Perform.,* Vol 12 (No. 3), 2003, p 244-248
9. M.B.D. Ellis, "Observation of Temper Embrittlement in 2.25Cr-1Mo Steel," Ph.D. Thesis, The University of Cambridge, 1986
10. T.L. Anderson, *Fracture Mechanics Fundamentals and Applications,* 2nd ed., CRC Press, 1996
11. C. Naudin, J.M. Frund, and A. Pineau, Intergranular Fracture Stress and Phosphorus Grain Boundary Segregation of a Mn-Ni-Mo Steel, *Scripta Mater.,* Vol 40, 1999, p 1013-1019
12. S. Suzuki, P. Lejeck, and S. Hofman, Effect of Metallurgical Factors on Grain Boundary Segregation of Solute Atoms in Iron, *Mater. Trans. JIM,* Vol 40 (No. 6), 1999, p 463-473
13. C.L. Briant and S.K. Banerji, Phosphorus Induced 350°C Embrittlement in an Ultra High Strength Steel, *Metall. Trans. A,* Vol 10A, 1979, p 123-131
14. G. Smith, A.G. Crocker, P.E.J. Flewitt, and R. Moskovic, *Damage and Failure of Interface,* H.K. Rossmanith, Ed., Balkema, 1997, p 229